International Journal of Engineering & Technology, 7 (2.24) (2018) 177-181

International Journal of Engineering & Technology

Website: www.sciencepubco.com/index.php/IJET

Research paper

Grid Integrated Solar Energy Conversion System Using Super-Lift Converter

Elangovan P[1*], Kamatchi[2], Nandhini[3], Kamaatchi Devi[4], Kokila[5]

[1,2,3,4,5]Department of Electrical & Electronics Engineering
Panimalar Institute of Technology, Chennai, India
**Corresponding Author E-mail: [1]elangoeee2007@gmail.com, [2]kamatchi.v25@gmail.com*

Abstract

Grid integrated photovoltaic (PV) system is capable of maximizing solar energy conversion by minimizing power losses. Conventionally, the grid integrated PV system uses boost or buck-boost DC-DC converters in the DC link for lifting up the PV output. Also, a separate complex circuit is used for active power compensation in the grid end. This paper proposes an advanced DC-DC converter by name Super-Lift Converter (SLC) in the DC link of grid integrated PV system. Unlike the conventional DC-DC converters, the proposed converter lifts up the DC link voltage thrice that of the input voltage. In addition, the proposed SLC is regulated using a PI controlled active front end (AFE) topology, which results in operation of unity power factor at grid end. The suggested system is simulated using MATLAB software. The presented results such as grid end voltage and current, input and output power of SLC and DC link voltage validates the effectiveness of the developed system.

Keywords: *Active Front End; DC-DC conversion; Energy; Photovoltaic; Voltage Ripple*

1. Introduction

In Modern days, solar energy is considered as one of the most reliable alternate for electrical power generation because it is environment friendly and daily available form of renewable energy [1]. Photovoltaic (PV) arrays are key equipment for capturing the solar power. The power generated in the PV panel is of a certain voltage level, which does not meet the grid requirement. The DC-DC Converter [2] plays a vital role to overcome the abovementioned problem. Though the DC-DC converters have more advantages, problems like duty cycle loss, high voltage ripple, complex control circuitry, etc., are still existing [3]. Several DC-DC converter topologies and control methods are discussed in the literature [4-7]. Those converters overcome the problems on output voltage ripple. But, the complex control topology and increased number of energy storage devices add disadvantages for those converters.

A study on high voltage gain boost converter involving zero voltage switching is presented in [8]. The main advantage of the proposed converter is it has reduced voltage stress across the main switch, which is very essential for renewable energy system. However, it suffers from power balancing issues. The power derived from PV panel is not constant throughout a day. Hence, it is necessary to tie the solar power with the grid power. Integrating the grid with PV leads to power quality issues at grid end. Therefore, an active power balancing circuit is required at the front end of the system. The topologies discussed in [9-12] eliminates additional power balancing circuits with the help of active power balance and it also reduces fluctuating neutral point currents using passive power balance.

On the other hand, maximum power point tracking (MPPT) approach using DC-DC converters is a trending research in the renewable energy conversion domain. For achieving MPPT, certain converters [13 & 14] interfaces sources of different voltage current characteristics with a load establishing high efficiency. Some strategies [15] use super capacitors as a constant voltage source and adapted to varying load conditions. This method reduces the charging and discharging pattern of the battery which decides fluctuation in PV and load power [16].

MPPT techniques has many algorithms by comparing there characteristics (Perturb & Observe, IC methods) are preferable [17 & 18].The tracking speed and accuracy gets varied for a different MPPT technique. Recently ,new Artificial intelligence(AI) methods are introduced to control the disadvantage of classical MPPT [19 & 20].these methods are used to identify the MPPT algorithm by artificial neural networks technique (ANN).thus the overall advantage of using MPPT are improved efficiency, increased running time, no frequent collapse of PV power.

This paper proposes a high efficient solar energy conversion system using Super-Lift Converter (SLC). The SLC is an advanced DC-DC converter belongs to the Luo converter series [21]. Conventionally, the system designed with PV panels use a boost converter in the DC link part, which maintains the output voltage only twice that of the input voltage and also, the ripple in the DC link voltage is more than 25%. The suggested work implements a SLC instead of boost converter. The proposed system has the following features:

- Efficient utilization of solar power.
- A DC-link voltage level 1.5 times greater than that of the conventional DC–DC converters.
- Ripple-free DC-link voltage and current.

2. Proposed System

The schematic of the proposed system is shown in Fig.1.

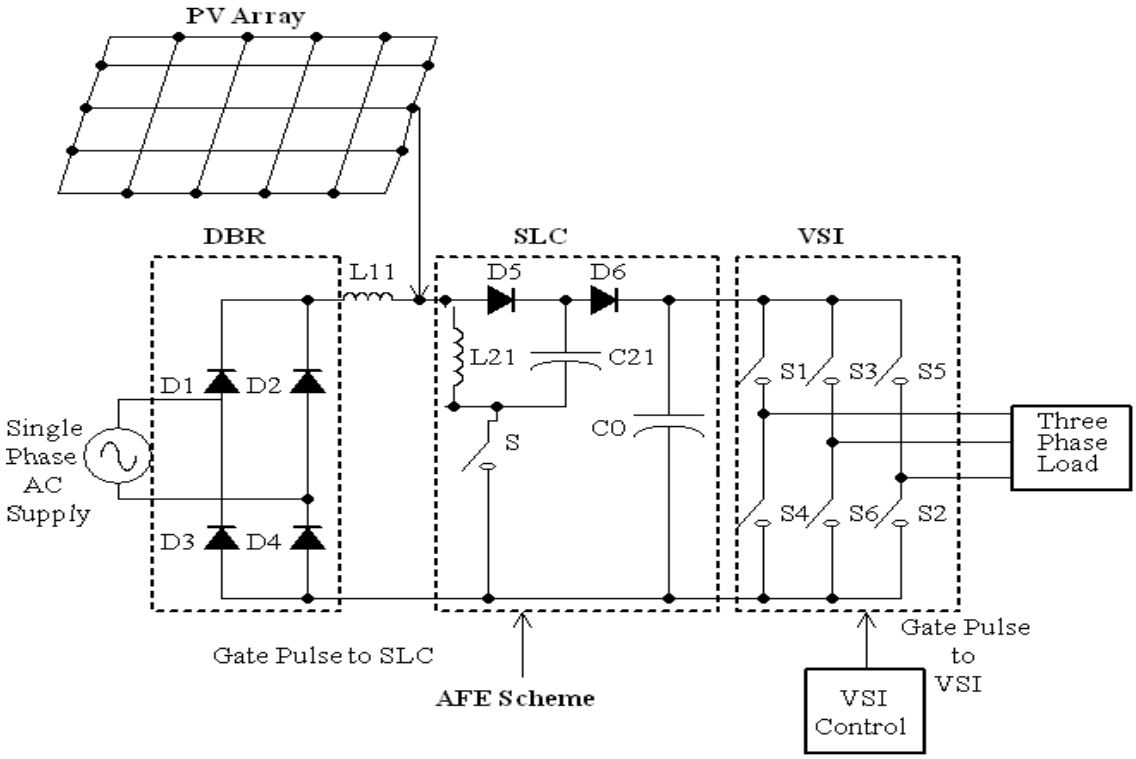

Fig. 1: Schematic of the proposed system

The complete system is divided into three stages. The first stage is to convert three phase AC power into fixed DC power using Diode Bridge Rectifier (DBR); the second stage is to convert the invariable DC power from DBR to variable DC using SLC and the last stage is to convert the DC power from SLC to variable voltage/variable frequency AC power using Voltage Source Inverter (VSI). In addition to the forward path, the PV array is integrated in the DC bus of the proposed model. Most PV based systems include a PV array, a DC bus capacitor, an intermediate DC-DC converter, a DC-AC inverter and an output filter. But, integrating PV based system with grid is a complicated one because; the power quality at the grid end is highly affected due to the injection of harmonics by the non-linear loads. The proposed scheme overcomes the above said problem by implementing a novel Active Front End (AFE) scheme at the DC link part along with the enhancement of maximum power point tracking (MPPT).

A. Working and Significance of SLC

The positive-output super-lift converters [22] is classified into five subseries and are the main, additional, enhanced, re-enhanced, and multiple-enhanced series. The elementary circuit from the main series, which is an immediate evolution of voltage lift converter, is implemented for the proposed system. The overall circuit of the SLC along with the equivalent circuit during switch ON and OFF is shown in Fig.2.

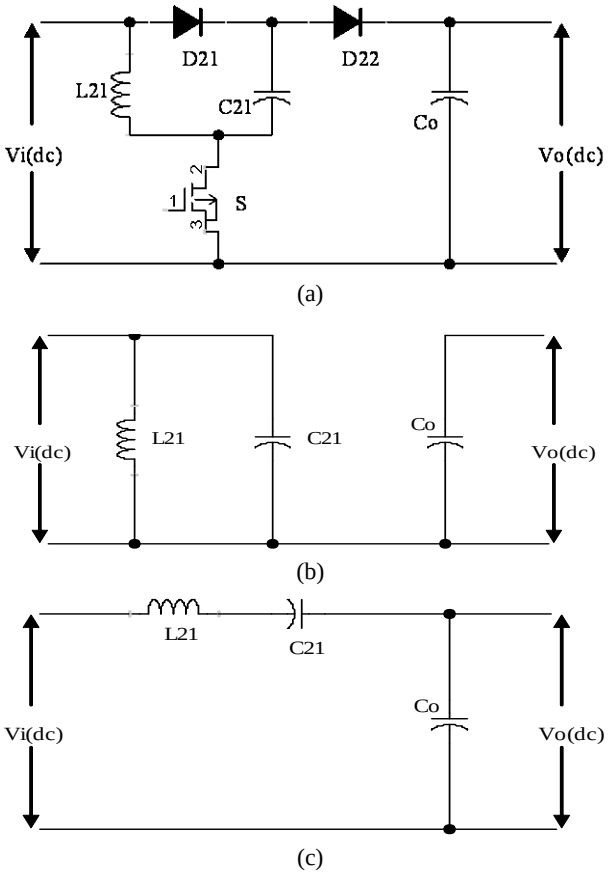

Fig. 2: (a) Overall circuit of the SLC, (b) SLC during switch ON, and (c) SLC during switch OFF

The input voltage to SLC from DBR charges the capacitor C_{21} to V_{idc}, during switch ON period and the current flowing through the inductor L_{21} raises with respect to V_{idc}. During switch OFF period of SLC, the capacitor C_{21} discharges and the current flowing through the inductor L_{21} reduces with $-(V_{odc}-2V_{idc})$.
The typical output voltage of the SLC is

$$V_{o(dc)} = \frac{2-\alpha}{1-\alpha} V_{i(dc)} \quad (1)$$

where, $V_{o(dc)}$ and $V_{i(dc)}$ are the output and the rectified input voltage of the ESLC. The output current of the SLC is given by,

$$I_{o(dc)} = \frac{1-\alpha}{2-\alpha} I_{i(dc)} \quad (2)$$

where, $I_{o(dc)}$ is the typical output current of the SLC, and $I_{i(dc)}$ is the input current of the SLC.
With respect to the firing angle (α) of SLC, the voltage transfer from DBR to VSI in terms of gain (G) is expressed as,

$$G = \frac{2-\alpha}{1-\alpha} \quad (3)$$

The voltage transfer gain of the conventional boost DC-DC converter in the proposed system is given by,

$$G = \frac{1}{1-\alpha} \quad (4)$$

On substituting the value of α = 0.5 in equations (3) and (4), the voltage transfer gain G for SLC is 3 and the voltage transfer gain G for boost converter is 2. This indicates that for the similar conduction duty, the SLC generates one and half times lifted voltage transfer than the conventional boost converter. The ripple content in the current flowing through the inductor "L_{21}" is expressed as,

$$\Delta i_{L21} = \left(\frac{V_{o(dc)} - 2V_{i(dc)}}{L_{21}} \right) T_{off} \quad (5)$$

where, T_{off} is the OFF time of the SLC.

B. Control Topology of SLC

The active front end topology using proposed super-lift converter is shown in Fig.3.

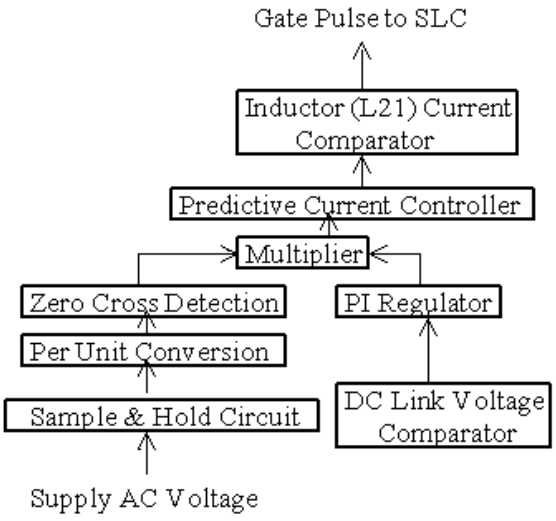

Fig. 3: Proposed AFE Scheme

Any one phase supply voltage is involved in this topology to generate the reference current for inductor L_{11}. The supply voltage is sampled using sample - hold circuit and converted to per unit (p.u.) form. The amplitude of negative half cycle in p.u. voltage waveform is shifted to positive half cycle using zero cross detection arrangement. The output of zero cross detection is multiplied with the PI controller output for producing the reference current of L_{11}. Here, the supply AC voltage is taken for generating the reference inductor (L_{11}) current and hence, the phase angle at which the voltage waveform follows will be equal to the phase angle of current waveform across the inductor (L_{11}). Thus, the achievement of zero phase difference between the supply voltage and current is validated. Finally, the error in the inductor (L_{11}) current is processed through the hysteresis current controller to generate the gate signal to SLC.

3. PI Controller Design for SLC

In the second path of the AFE scheme, the actual DC link voltage which is the output voltage of SLC is compared with the reference DC link voltage and the error is processed by the proportional plus integral (PI) controller. The control action of PI regulator is dependent on the proportional time constant (K_P) and the integral time constant (T_I). The values of K_P and T_I are determined by using Ziegler-Nichol's tuning method [23].
According to the Ziegler-Nichol's tuning method, the values of K_P and T_I are calculated from the delay time constant L and the time constant T, which are observed from the step response S-shaped curve of SLC. To attain the S-shaped curve, the state space model of the SLC [24 & 25] is to be developed.
The state space model of SLC is determined by assuming the state variables P_1 (current flowing through L_{21}), P_2 (voltage across C_{21}) and P_3 (Voltage across C_O). Neglecting the input and the output resistance of the suggested SLC, the state space equation of SLC during switch ON period is given by,

$$\begin{bmatrix} \dot{P_1} \\ \dot{P_2} \\ \dot{P_3} \end{bmatrix} = \begin{bmatrix} 0 & 0 & 0 \\ \frac{-1}{C_{21}} & 0 & 0 \\ 0 & 0 & \frac{-1}{C_0} \end{bmatrix} \begin{bmatrix} P_1 \\ P_2 \\ P_3 \end{bmatrix} + \begin{bmatrix} \frac{1}{L_{21}} \\ \frac{1}{C_{21}} \\ 0 \end{bmatrix} u \quad (6)$$

where, u is the input variable (i.e.,) input voltage of SLC.
The state space equation of SLC during switch OFF period is given by,

$$\begin{bmatrix} \dot{P_1} \\ \dot{P_2} \\ \dot{P_3} \end{bmatrix} = \begin{bmatrix} 0 & \frac{-1}{L_{21}} & \frac{-1}{L_{21}} \\ \frac{-1}{C_{21}} & 0 & 0 \\ \frac{-1}{C_0} & 0 & \frac{-1}{C_0} \end{bmatrix} \begin{bmatrix} P_1 \\ P_2 \\ P_3 \end{bmatrix} + \begin{bmatrix} \frac{1}{L_{21}} \\ 0 \\ 0 \end{bmatrix} u \quad (7)$$

The averaging state space model of the proposed SLC is expressed as,

$$\begin{bmatrix} \dot{P_1} \\ \dot{P_2} \\ \dot{P_3} \end{bmatrix} = \begin{bmatrix} \frac{1}{L_{21}} & \frac{\alpha-1}{L_{21}} & \frac{\alpha-1}{L_{21}} \\ \frac{1-2\alpha}{C_{21}} & \frac{-\alpha}{C_{21}} & 0 \\ \frac{1-\alpha}{C_0} & 0 & \frac{1}{C_0} \end{bmatrix} \begin{bmatrix} P_1 \\ P_2 \\ P_3 \end{bmatrix} + \begin{bmatrix} \frac{1}{L_{21}} \\ \frac{\alpha}{C_{21}} \\ \frac{1}{C_0} \end{bmatrix} u \quad (8)$$

Now, applying step input for the overall state model of SLC represented in equation (8), the S-shaped curve is achieved and is shown in Fig.4. By drawing a tangential line over the S-shaped curve, the delay time constant (L=0.05s) and the time constant (T=0.052s) are observed. The values of K_P (9.36) and T_I (0.016) are straight away taken from the Zeigler-Nichol's tuning chart for the corresponding values of L and T. The PI regulator with the determined constants will eliminate the error in the DC link voltage.

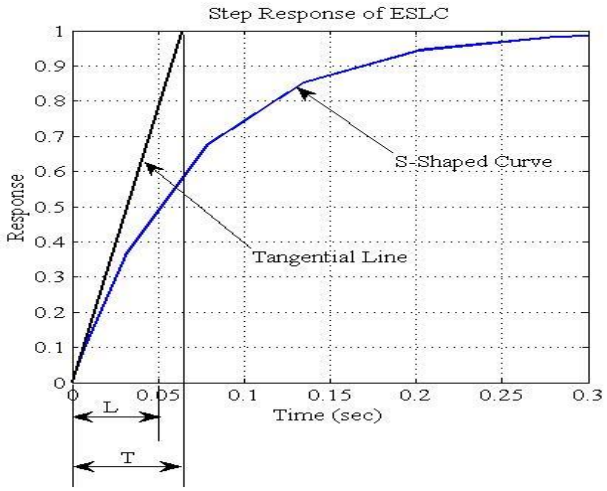

Fig. 4: Step Response of ESLC

Finally, the signals from both the parallel paths are multiplied to generate the reference current for the inductor L_{21}. The reference and the actual current passing through the inductor $L_{21}$is compared and the error is processed by the hysteresis current controller to produce the gate signal for SLC.

4. Results and Discussion

To validate the effectiveness of the proposed scheme, the Simulink model of SLC-based grid integrated solar energy conversion system is designed. The simulation is conceded by using MATLAB 2012a software. The simulation circuit parameters are presented in Table 1.

Table 1: Parameters of Simulink Model

PARAMETER	RATING
Grid Input AC supply	1 phase, 100 V, 50 Hz
Capacity of Solar Panel	100 W
inductors	L_{11} = 3 mH, L_{21} = 2.56 mH
capacitors	$C_{21} = C_o$ = 2000 µF
Voltage Source Inverter (VSI)	insulated-gate bipolar transistor

The simulation result on utility end voltage and current in the absence of the proposed AFE control is shown in Fig.5. It is very clear that, the utility end PF is very poor in the absence of proposed AFE control and also the line current is extremely distorted. In the presence of proposed AFE control, the simulation result on utility end voltage and current is attained and is shown in Fig.6. The voltage and current waveform has the same, which indicates the operation of the proposed drive with unity PF at utility end.

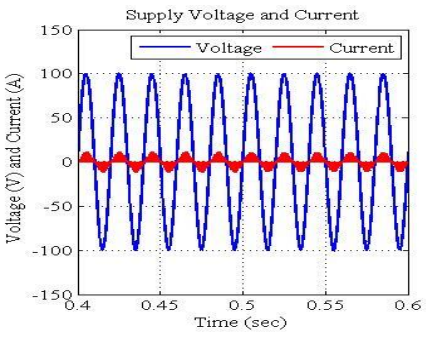

(a)

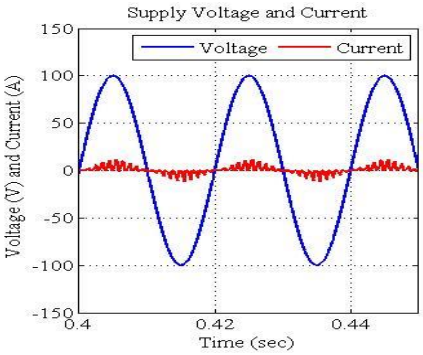

(b)

Fig. 5: Utility end Voltage and Current without the proposed AFE (a) actual (b) zoomed

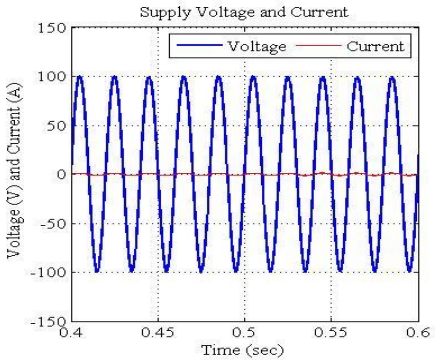

(a)

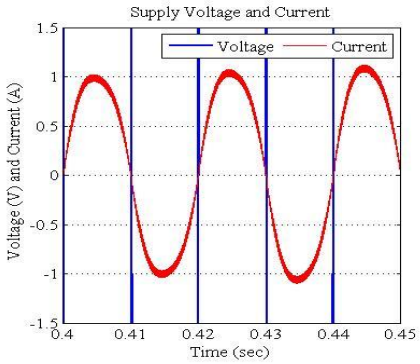

(b)

Fig. 6: Utility end Voltage and Current with the proposed AFE (a) actual (b) zoomed

To validate the impact of SLC in solar energy conversion system, the input power from PV array and the output power from SLC is observed and shown in Fig. 7.

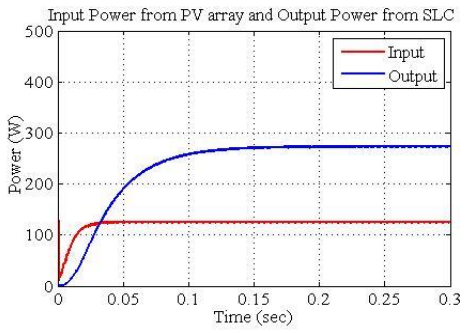

Fig. 7: Input Power from PV array and output Power from SLC

The result shown in Fig.7 authenticates that the presence of SLC pumps up the DC link power three times than that of the input power. Also, the ripple content in the voltage signal is less than 1%.

To show the superiority of SLC in the voltage pump up aspect, the DC link voltage with respect to PV output voltage is attained and shown in Fig. 8.

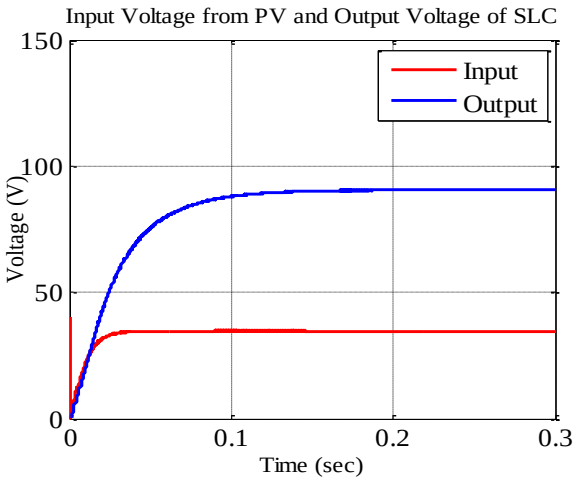

Fig. 8: Input Voltage from PV and Output Voltage of SLC

The result shown in fig. 8 depicts that the presence of SLC in DC link maintains the voltage ripple less than 1%. In addition, the DC link voltage is lifted from 25V to 75V.

5. Conclusion

A Grid integrated PV system using SLC is presented in this manuscript. The AFE control in this system works on prognostic algorithm and the impact of the projected AFE control on grid end and DC link part are deliberated. A comparison between the utility end voltage-current with and without the suggested AFE is analyzed through simulation. The results point out that the utility end PF is unity for grid integrated PV system with the suggested AFE, whereas the utility end PF is less than 0.5 in the nonappearance of the amended AFE control. The ability to reduce DC link voltage ripple less than 1% and the lift-up of DC link voltage level three times that of the PV voltage are the major advantages of amended SLC, which sorts it as a suitable substitute for the traditional boost DC–DC converters in the solar energy conversion system.

References

[1] Farzam Nejabatkhah, ”Modeling and control of new three input dc-dc boost converter for hybrid PV FCL battery power system,” IEEE Transaction on power electronics., vol. 27, no. 5, May 2012.

[2] Monzer Al Sakka , Joeri Van Mierlo and HamidGualous ,”DC-DC converter for electric vehicles,” VRIJI universiteitBrussel, Universite de Caen Basse-Normandie Begium ,France.

[3] K.V Ravi Kishore, B.Wang, Z.Wang and PL.SO,”Design and implementation of APWM ZVZCS full bridge DC-DC converter for battery charging in EV,” IEEE Transaction on power electronics., Sep 14 2016.

[4] B. Whitaker, A. Barkley, Z. Cole, B. Passmore, D. Martin, T. R. McNutt, A. B. Lostetter, J. S. Lee and K. Shiozaki, “A high-density, high-efficiency, isolated on-board vehicle battery charger utilizing silicon carbide power devices,” IEEE Trans. Power Electronics, vol. 29, no. 5, pp. 2606-2617, May 2014.

[5] A. Khaligh and S. Dusmez, “Comprehensive topological analysis of conductive and inductive charging solutions for plug-in electric vehicles,” IEEE Trans. Vehicular Technology, vol. 61, no. 8, pp. 3475- 3489, Oct. 2012.

[6] Z. Chen, L. Shi, and F. Ji, “Comparison of phase-shifted full-bridge converters with auxiliary networks,” in Proc. International Power Electronics and Motion Control (IPEMC), 2012, pp. 1700-1706.

[7] B. Yang, J. L. Duarte, W. Li, K. Yin, H. Xiangning, and Y. Deng, “Phase-shifted full-bridge converter featuring ZVS over the full-load range,” in Proc. IEEE Annual Industrial Electronics Conference (IECON), 2010, pp. 644-649.

[8] Luiz Henrique S. C. Barreto,” High-Voltage Gain Boost Converter Based on Three-State Commutation Cell for Battery Charging Using PV Panels in a Single Conversion Stage,” IEEE Trans. Power Electronics,vol.29,NO.1,Jan 2014.

[9] Longcheng Tan,” Comprehensive DC Power Balance Management in High-Power Three-Level DC-DC Converter for Electric Vehicle Fast Charging,” IEEE Trans. Power Electronics, vol. 28, no. 9, Mar 2015.

[10] B. Wu, “High-power converters and ac drives,” IEEE Press-Wiley., 2006.

[11] J. Rodriguez, S. Bernet, P. K. Steimer, and I. E. Lizama, “A survey on neutral-point-clamped inverters,” Industrial Electronics, IEEE Transactions on, vol. 57, no. 7, pp. 2219–2230, 2010.

[12] J. Yang, F. C. Lee, and L. Sizhao, “Space Vector Modulation for Three-Level NPC Converter With Neutral Point Voltage Balance and Switching Loss Reduction,” IEEE Trans. Power Electron., vol. 29, no. 10, pp.5579–5591, 2014.

[13] Jianwu Zeng, ”An Isolated Three-Port Bidirectional DC-DC Converter for Photovoltaic Systems with Energy Storage,” IEEE Trans. Power Electron., vol.5,Jan 2015.

[14] J. Lee, B. Min, D. Yoo, R. Kim, and J. Yoo, “A new topology for PV DC/DC converter with high efficiency under wide load range,” in Proc. European Conf. Power Electron. Appl., Sept. 2007, pp. 1-6.

[15] Fariborz Musavi, ”Control Strategies for Wide Output Voltage Range LLC Resonant DC-Dc Converters in Battery Chargers,” IEEE Transactions on Power Electronics, Jan 2014.

[16] T. Liu, Z. Zhou, A. Xiong, J. Zeng, and J. Ying, “A novel precise design method for LLC series resonant converter,” in Proc. IEEE INTELEC, 2006, pp. 1–6.

[17] D. Casadei , G. Grandi and C. Rossi, “Single-phase single stage PV generation system based on a ripple correlation control maximum power point tracking,” IEEE Trans. on Energy conversion, 2006.

[18] S.Liu, H.Liu and Y.Zha, "A solar maximum power point tracking algorithm based on a discrete-time ripple correlation control" Transaction of the Chinese Society of Agriculture Engineering, 2013.

[19] Bouzelata Yahia, Djeghloud HIND,Chenni Rachid,"The application of an active power filter on a PV power generation system,” International journal of renewable energy research., vol. 2, 2012.

[20] Hanen Abbes, Hafedh Abid, Kais Loukil,"An Improved MPPT incremental conductance algorithm using T-S fuzzy system for PV panel '"International journal of renewable energy research ,vol. 5, 2015.

[21] Luo F.L and YeH., Advanced DC-DC converters CRC press, chapter 3, 2003.

[22] Luo F.L. and Ye H., “Positive output super-lift converters,” IEEE Transaction on Power Electronics, vol. 18, no. 1, pp.105-113, 2003.

[23] Comines. P and Munro.N., “PID Controlers recent tuning methods and design of specifications,” Proceeding of IEEE control theory and applications, vol. 149, no. 1,pp. 46-53, 2002.

[24] Mattavelli P., Rossetto L. and Spiazzi G., “Small signal analysis of DC-DC converter with sliding mode control,” IEEE Transactions on Power Electronics, vol. 12, no. 1, pp. 96-102, 1997.

[25] Panov Y., Rajagopalan J., and Lee F.C., “Analysis and control design of N paralleled DC-DC converters with master-slave current sharing control,” in Proceeding of Applied Power Electronics Conference, pp. 436-442, 1997.

[26] M. Rajesh, Manikanthan, “ANNOYED REALM OUTLOOK TAXONOMY USING TWIN TRANSFER LEARNING”, International Journal of Pure and Applied Mathematics, ISSN NO: 1314-3395, Vol-116, No. 21, Oct 2017.

[27] T.Padmapriya and V.Saminadan, “Utility based Vertical Handoff Decision Model for LTE-A networks”, International Journal of Computer Science and Information Security, ISSN 1947-5500, vol.14, no.11, November 2016.